Effect of high temperature on the microstructural evolution of fiber reinforced geopolymer composite

Sneha Samal *

Institute of Physics of the Czech Academy of Sciences, Na Slovance 2, 182 21 Praha 8, Czech Republic

A B S T R A C T

Physical evolution of geopolymeric minerals derived from metakaolin and synthesized with sodium, mixed-alkali and potassium activating solutions (Na- K) during thermal exposure. The geopolymer composites were prepared with 40 V% of fiber reinforcement such as carbon, E-glass, and basalt at the direction of in plain. Fiber reinforced geopolymer composites were exposed to the room and elevated temperatures inside the oven at air medium for a period of 30 min. The durability of the composites and internal structures with surface microstructures were examined after high temperature exposures. According to the results, geopolymer implied a prominent influence on the thermal shrinkage with the increasing of Si/Al ratios. This was attributed to the densification caused by reduction in porosity during dehydroxylation and sintering. In the case of carbon fiber reinforced composite shows transition in strength after 600 °C due to the oxide protective layer that increases the flexural strength and toughness of the composite. The flexural strength of the carbon reinforced composite increases from 17.8 to 55.8 MPa at 1000 °C. Whereas, E-glass reinforced composite shows expansion in a matrix with cage like structure helps in the sliding mechanism of fiber within the matrix, thus strength reduces towards high temperature. In case of basalt reinforces composite complete conversions into a ceramic like structure after exposure to high temperature. As a result, the crystalline nature of ceramic assists in toughened the composite structure with a brittle nature.

1. Introduction

Fiber reinforced geopolymer composite open up wide space in construction and building industries, with substituting cementitious material. The material suitability of geopolymer also adds benefits on the basis of fire proofing characteristics [1, 2]. New inorganic fire-resistant polymer materials which called "geopolymers". The invention of mineral geopolymers of the types poly (Si-O) -Si-O-Al-O- (Si:Al = 1), poly (Si-O-Al) -Si-O-Al-O-Si-O- (Si:Al = 2), poly (Si-O-Al) -Si-O-Al-O-Si-O--Si-O- (Si:Al = 3), (Si:Al>>3) stands in catastrophic fires rather than common organic plastic, research on non-flammable and non-combustible plastic materials became priority [3, 4]. The material can exposure to fire for certain finite duration of time without emission of CO_2, and other hazardous gaseous to the surrounding [5]. This novelty opens up new possibilities of investigation on geopolymer materials and its withstanding behavior towards high temperature [6, 7]. Physical evolution of geopolymeric minerals derived from metakaolin and synthesized with sodium, mixed-alkali and potassium activating solutions (Na- K) during thermal exposure. According to the results, geopolymer implied prominent influence on the thermal shrinkage with the

increasing of Si/Al ratios. This was attributed to the densification caused by reduction in porosity during dehydroxylation and sintering. In addition, as geopolymer shows lower mechanical strength, however, fiber reinforced geopolymer shows an increase in flexural strength and its properties changes as the function of temperature [8]. As a result, on a combination of both properties of geopolymer towards fire resistance and flexural strength, it's essential to investigate the behavior of fiber reinforced geopolymer composite towards high temperature [9, 10]. The strength of the carbon fiber reinforced composite is maximum at 65 MPa observed at room temperature [11, 12]. However, the fire proofing behavior of geopolymer matrix and sustainability of fiber is the subject of allows understanding the behavior of fiber, matrix, fiber-matrix interaction, adhesion as the function of temperature and its contribution towards the final strength of the composite. The durability of the fiber reinforced composite was revealed using impact analysis and its residual strength after the impact [13, 14]. Damage tolerance of the fiber reinforced composite was revealed during exposure to elevated temperatures [15, 16]. The correlation between strength and high temperature exposure was well presented in the fiber reinforced geopolymer composite [17, 18, 19]. However, the brief explanation about the individual role of

---

* Corresponding author.
  E-mail address: samal@fzu.cz.

Table 1
Fabrication of geopolymer matrix, fiber and fiber reinforced composites.

Composites reinforcement with fiber	Density g/cm^3	Fiber V fraction %	Matrix V fraction %	Voids V fraction %
Carbon	1.51	39	40	21
E-glass	1.80	41	37	22
Basalt	1.97	40	45	15

fiber within the matrix is lacking in this area after exposure to elevated temperatures.

To reveal the unusual strength increase at high temperature in case of carbon fiber, an investigation was carried out in depth on the basis of microstructural changes after exposure to high temperature. The role of fiber adhesion and its microscopic changes were evaluated at each step for composites at various temperature. The microstructural evolution, matrix transformations, and fiber sustainability within the composite at

high temperature is examined carefully. Herewith, there is an open possibility arises to study, investigate and examine the fiber reinforced geopolymer composite sustainability at high temperature. The evolution of physical, structural changes in terms of density The evolution in microstructural features, fiber, matrix geopolymer, the adhesion strength of composite studied carefully and interpret the result in constructive ways. The various temperature starting from room temperature (RT) towards high temperature up to 1300 °C until the final breakage of geopolymer composite is investigated. The phase structure, evolution of adhesion, fiber, matrix at each temperature is investigated and interpreted for the overall residual strength of the composite after heat treatment. The rule of mixture for the composite in terms of fiber and matrix and voids were taken into consideration and overall contribution after each temperature treatment is presented in this article with a combination of micro structural images. The present special issue, acknowledging the scarcity of publications on reinforced geopolymer-composites, for the understanding of geopolymer resins, binders/

Table 2a
Physical and mechanical properties of fiber reinforced geopolymer composite.

Physical properties (RT)	Matrix	fiber			Composite (RT)		
		C	E-glass	Basalt	C	E-glass	Basalt
Density (g/cm3)	2.0	1.7	2.6	2.7	1.63	1.95	1.88
Composition	Si: Al = 15.6	C > 99.9 wt. %	SiO$_2$:54 Wt%, Al$_2$O$_3$:14 Wt%, CaO + MgO:22 Wt%, B$_2$O$_3$:10 Wt%	SiO$_2$≈50 Wt%, CaO, Na$_2$O, FeO, Al$_2$O$_3$	C > 99.9 wt. %	SiO$_2$:54 Wt%, Al$_2$O$_3$:14 Wt%, CaO + MgO:22 Wt%, B$_2$O$_3$:10 Wt%	SiO$_2$≈50 Wt%, CaO, Na$_2$O, FeO, Al$_2$O$_3$
Flexural/tensile strength (MPa)	18.5	282	129	219	192	70.9	39.7
Flexural/tensile modulus	27.8	25.1	19.6	24.2	12.5	9.0	10.7
Failure strain	0.44	1.32	1.51	1.26	2.4	2.9	0.73

Table 2b
Physical and mechanical properties of fiber reinforced geopolymer composite at elevated temperature (600 and 1000 °C).

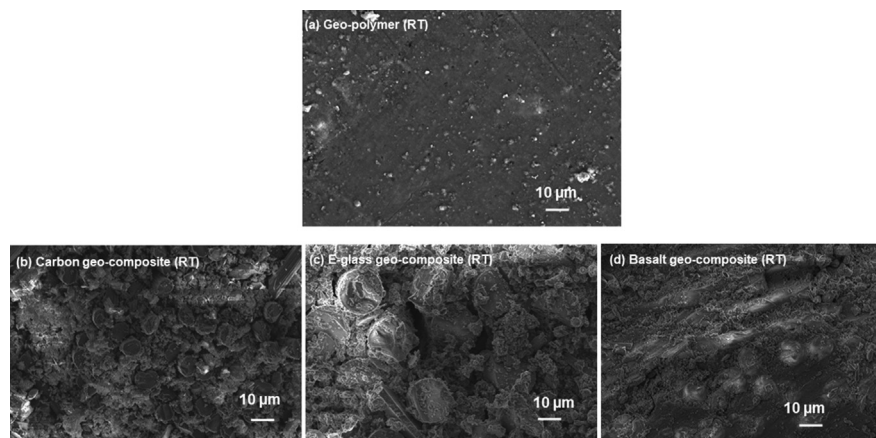| Physical properties (RT)	Composite (T600>>RT)			Composite (T1000>>RT)		
Fiber	C	E-glass	Basalt	C	E-glass	Basalt
Density (g/cm3)	1.1	0.77	1.07	1.13	0.65	0.73
Composition	C > 99.9 wt. %	SiO$_2$:54 Wt%, Al$_2$O$_3$:14 Wt%, CaO + MgO:22 Wt%, B$_2$O$_3$:10 Wt%	SiO$_2$≈50 Wt%, CaO, Na$_2$O, FeO, Al$_2$O$_3$	C > 99.9 wt. %	SiO$_2$:54 Wt%, Al$_2$O$_3$:14 Wt%, CaO + MgO:22 Wt%, B$_2$O$_3$:10 Wt%	SiO$_2$≈35 Wt%, CaO, Na$_2$O, FeO, Al$_2$O$_3$
Flexural/tensile strength (MPa)	17.8	9.3	8.3	55.8	5.3	-
Flexural/tensile modulus	1.5	3.0	2.0	10.7	2.9	-
Failure strain	1.3	0.81	0.57	0.79	0.71	-

Fig. 1. (a) Geopolymer matrix at room temperature and (b–d) fiber reinforced geopolymer composite with carbon, E-glass and basalt at room temperature.
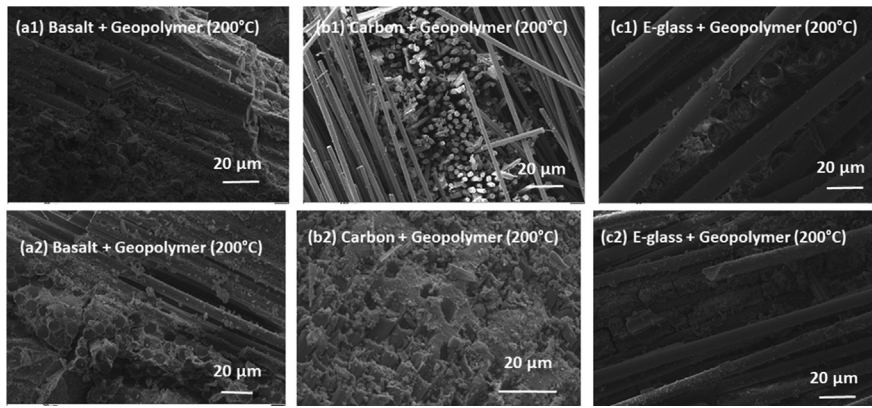
Fig. 2. (a1–a2) Basalt fiber reinforced geopolymer composite after exposure to 200 °C at two different location showing adhesion and ceramic structure conversion. (b1–b2) Carbon fiber reinforced geopolymer composite after exposure to 200 °C at two different location showing distribution of fibers and adhesion. (c1–c2) E-glass fiber reinforced geopolymer composite after exposure to 200 °C at two different location showing adhesion.
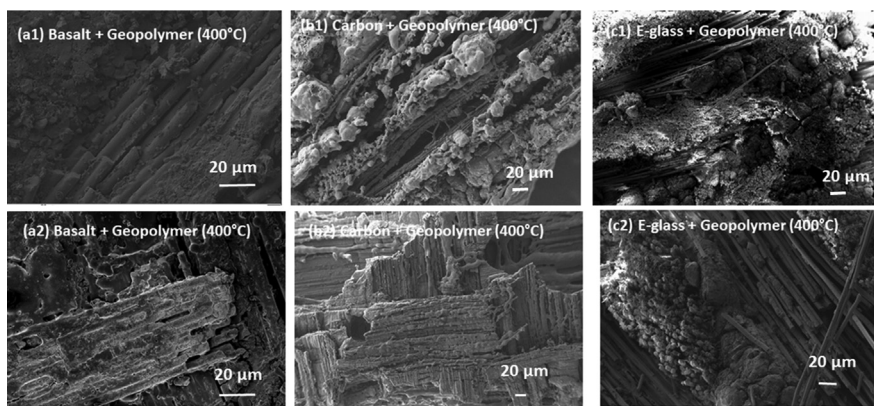

Fig. 3. (a1–a2) Basalt fiber reinforced geopolymer composite after exposure to 400 °C at two different location showing ceramic structure conversion. (b1–b2) Carbon fiber reinforced geopolymer composite after exposure to 400 °C at two different location showing necking of matrix connection within fiber and its alignment direction. (c1–c2) E-glass fiber reinforced geopolymer composite after exposure to 400 °C at two different location showing packing of matrix within interspace region of fibers.
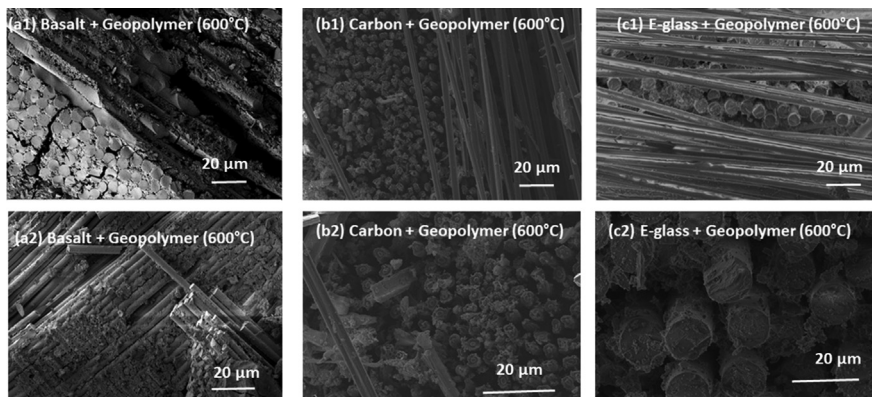

Fig. 4. (a1–a2) Basalt fiber reinforced geopolymer composite after exposure to 600 °C at two different location showing cracks and porous ceramic structure. (b1–b2) Carbon fiber reinforced geopolymer composite after exposure to 600 °C at two different location showing disintegration of fibers and breakage in some region. (c1–c2) E-glass fiber reinforced geopolymer composite after exposure to 600 °C at two different location showing expansion in longitudinal and transverse direction.

cement and reinforcement fiber properties at elevated temperature. In this work, an investigation was carried out on the microstructural evolution in 3D inner view of the composite as well as surface features of the fiber reinforced composite at elevated temperature.

Here an overall feature of microstructure evolution after high temperature exposure and its 3D inner view of the structures has been examined by micro computed tomography. The surface microstructure evolution of fiber reinforced geopolymer composites as the function of various temperature has been examined briefly. The detail in step for each categorized of temperature exposure is evaluated in terms of fiber adhesion, matrix shrinkage and fiber –matrix interaction as the function of exposing temperature.

2. Materials and methods

2.1. Fibers and matrix

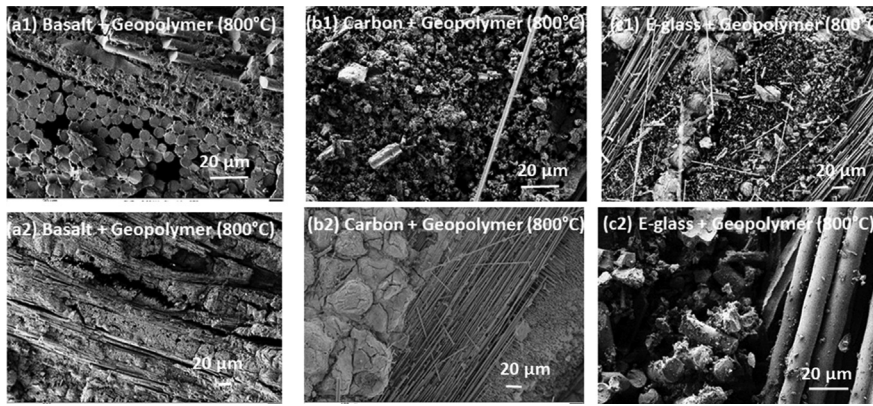Three various types of fibers such as carbon, E-glass, and basalt were

Fig. 5. (a1–a2) Basalt fiber reinforced geopolymer composite after exposure to 800 °C at two different location showing micro porous structure. (b1–b2) Carbon fiber reinforced geopolymer composite after exposure to 800 °C at two different location showing more packing regions. (c1–c2) E-glass fiber reinforced geopolymer composite after exposure to 800 °C at two different location showing breakage of fibers.
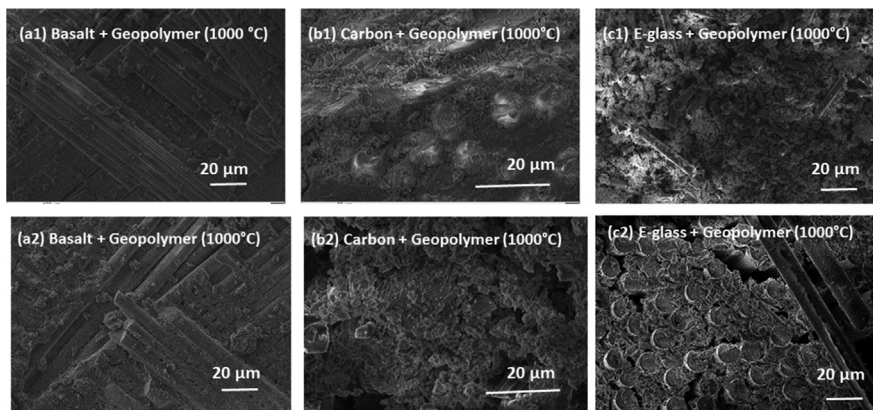

Fig. 6. (a1–a2) Basalt fiber reinforced geopolymer composite after exposure to 1000 °C at two different location showing complete conversion in ceramic. (b1–b2) Carbon fiber reinforced geopolymer composite after exposure to 1000 °C at two different location shows a compact structure of coating of white oxide layers. (c1–c2) E-glass fiber reinforced geopolymer composite after exposure to 1000 °C at two different location showing cracks and gaps.
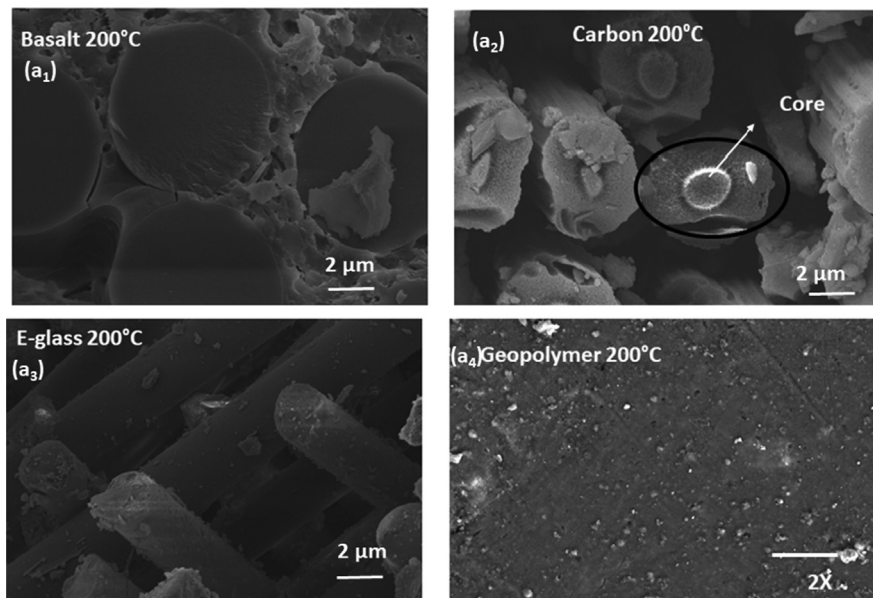

Fig. 7. (a1–a4) Fibers such as basalt, carbon, E-glass and matrix evolution at 200 °C showing initial fiber evolution.

considered as in direction of in plain for the fiber reinforced geopolymer composite materials. Geopolymer matrix such as alumino-silicate with metakaolin binder is considered as raw material for the composite material. Geopolymer matrix was prepared with metakaolin (6.88%), alumino-silicate powder (49%) and alkali activator with the NaOH/KOH (44.12%) content ratio of 15:6 supplied by the Research institute of inorganic chemistry Inc., Czech Republic. The elemental chemical composition of geopolymer in percentage is shown as Al (2.04), Si
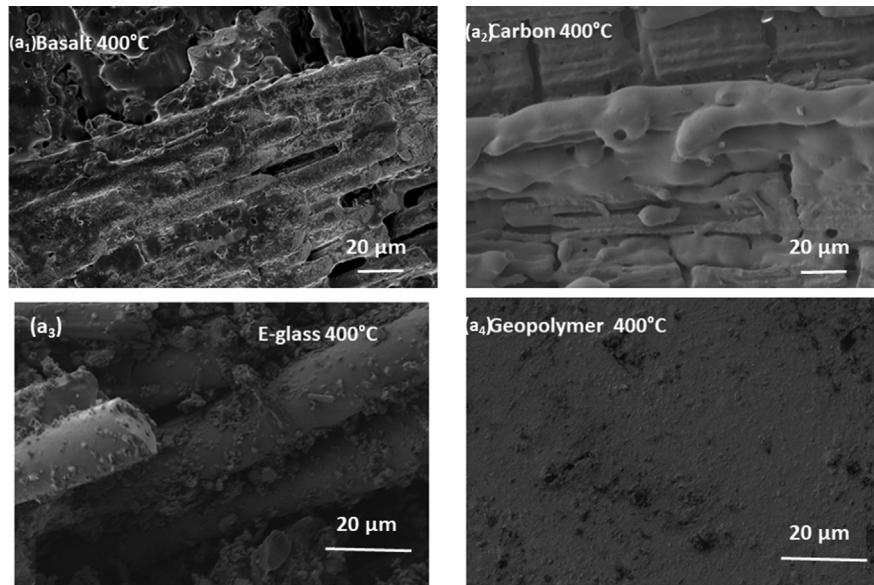
Fig. 8. (a1–a4) Fibers such as basalt, carbon, E-glass and matrix evolution at 400 °C showing necking of matrix flow within fiber.
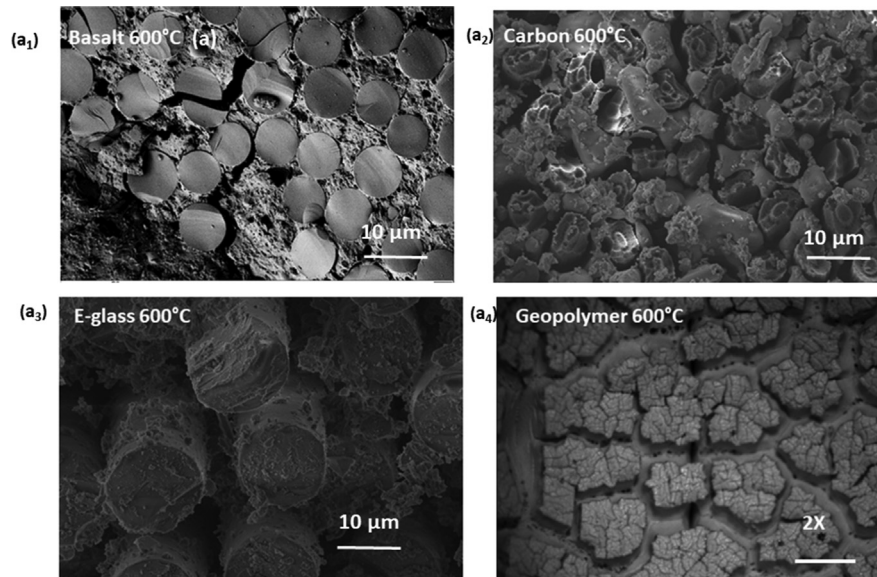

Fig. 9. (a1–-a4) Fibers such as basalt, carbon, E-glass and matrix evolution at 600 °C showing non adhesion of fibers region, micro and mini cracking regions of matrix.

(31.80), P (0.08), K (15.5), Zr (1.76), Na (0.63), Ca (0.24) and O (48.32). The geo-polymer (matrix) was initially prepared by mixing Al: Si powder, metakaloin and alkali activator solution for 10 min to obtain the homogenous mixture. The volume fraction of 40 V. % of fabrics was manually filled by geopolymer mix, stacked together in the identical direction, compressed by a roller till the desired thickness of about 3 mm was achieved. The assembled fabric reinforced geo-polymer composites were placed in a vacuum bag and cured at 0.003 MPa at ambient temperature for 2 h. The bag was then placed in a curing oven at 70 °C for a period of 2 h, and finally, the samples were cured inan air environment for 20 h at ambient temperature. Table 1 shows the fabrication of composite with various fibers and their respective volume fraction of matrix, fibers and voids content. Physical properties of the geopolymer, fibers, and fiber reinforced composites are displayed in Tables 2a and 2b at room and elevated temperature. In the overall composite material, fiber, matrix, voids have a significant contribution towards the final material in terms of mass density, ultimate flexural strength, elastic modulus and thermal conductivity of the material. Fibers such as carbon, E-glass, and basalt shows the maximum flexural strength and young modulus with strain at various temperature. Composite samples ($100 \times 100 \times 3$ mm^3) were prepared, by hand lay-up technique, with fabrics of carbon, E-glass and basalt reinforcement in alumino-silicate geopolymer matrices with metakaolin binders, using piles of fabrics in the 0–90° direction [10]. The assembled fabric reinforced geopolymer composites were placed in a vacuum bag and cured, at 0.003 MPa and room temperature, for 24 h. The bag with composite was then placed in a curing oven at 70 °C for 12 h [10]. To maintain a thickness of 3 mm, the fabrics were arranged in different layers, such as 7 layers of E-glass, 10 layers of carbon and 15 layers of basalt fabric. The volume fraction of fiber, matrix, and voids of the three laminates was calculated according to the formulas reported in Eqs. (1), (2), and (3) and their values are reported in Table 1
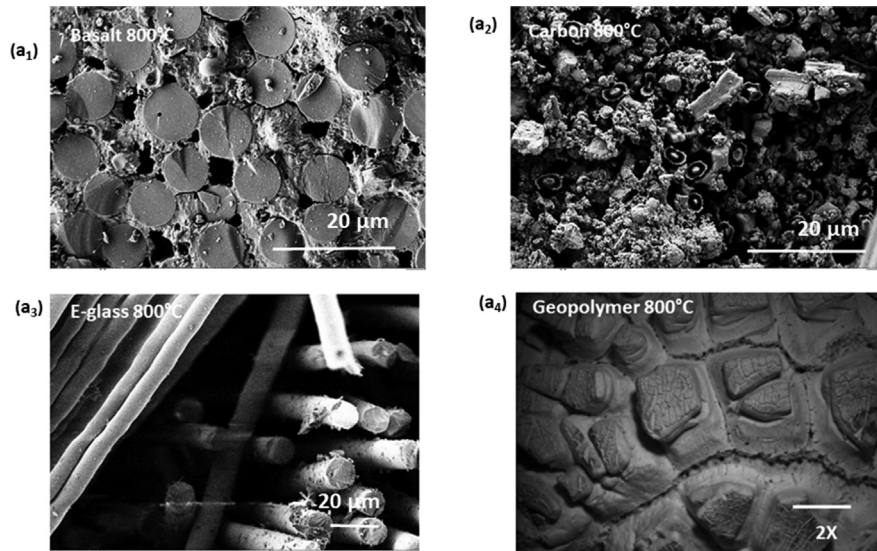
Fig. 10. (a1–a4) Fibers such as basalt, carbon, E-glass and matrix evolution at 800 °C showing micro voids, disintegration of carbon fibers, voids in E-fibers and micro crack regions of matrix.
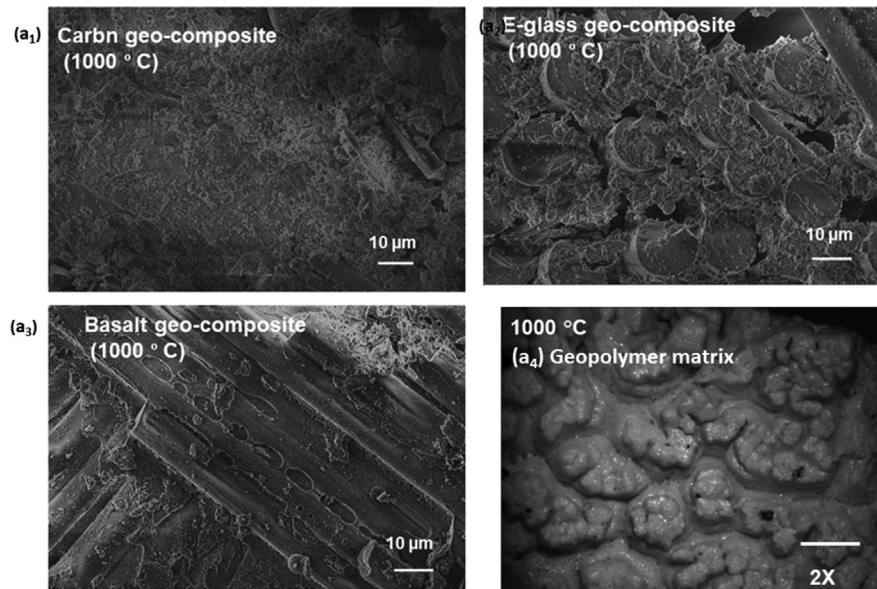

Fig. 11. (a1–a4) Fibers such as basalt, carbon, E-glass and matrix evolution at 1000 °C showing oxide layers of carbon fiber, expansion of E-glass fiber, ceramic nature of basalt and melting of matrix.

$$V_f = \frac{n\rho_w}{t\rho_f} \cdot 100\% \tag{1}$$

$$V_m = \frac{1}{t\rho_m} \left[\frac{m_c}{Lb} - n\rho_w \right] \cdot 100\% \tag{2}$$

$$V_v = 100 - \left(V_f + V_m \right) \tag{3}$$

where V_f, V_m, V_v are volume fractions of fibers, matrix, and voids in a sample

n is number of fiber layers in a composite sample

t, L, b are thickness, length, width of a composite sample

m_c is mass of a composite sample

ρ_w is density of fiber layer, mass per unit of area

ρ_f is density of single fiber, mass per unit of volume

ρ_m is density of matrix, mass per unit of volume

The fabric reinforced geopolymer composites ($3 \times 14 \times 90$ mm^3) were exposed to heat in an electric furnace with the radiant heat source 25 kW/m^2. After the heating to a chosen temperature of the range from 200 to 1000 °C and a holding time of 30 min, the samples were cooled down in the air to room temperature.

2.2. Surface feature of geopolymer composite

Microstructural evolution of fiber reinforced geopolymer is explained by surface features like the function of temperature [19]. The resistance of fiber, matrix, adhesion bonding between fiber and matrix in a composite structure is well examined in surface morphology. The fiber rupture, matrix cracks, evolution of non-adhesion between fiber and matrix with respect to temperature is predicted by the surface morphology of the composite. The cross section of the sample was carried out after heat exposure and then examined under scanning electron
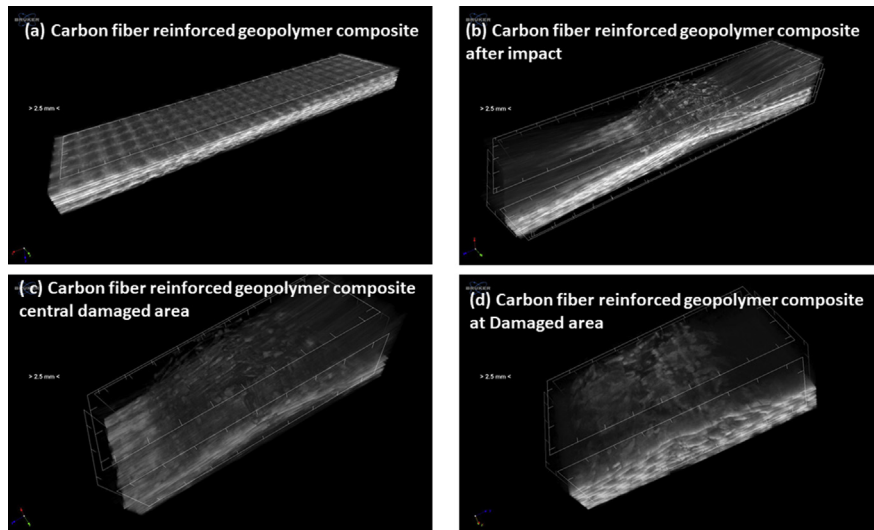
Fig. 12. (a–d) 3D image of the carbon fiber reinforced composite and damaged carbon composite at various stage.
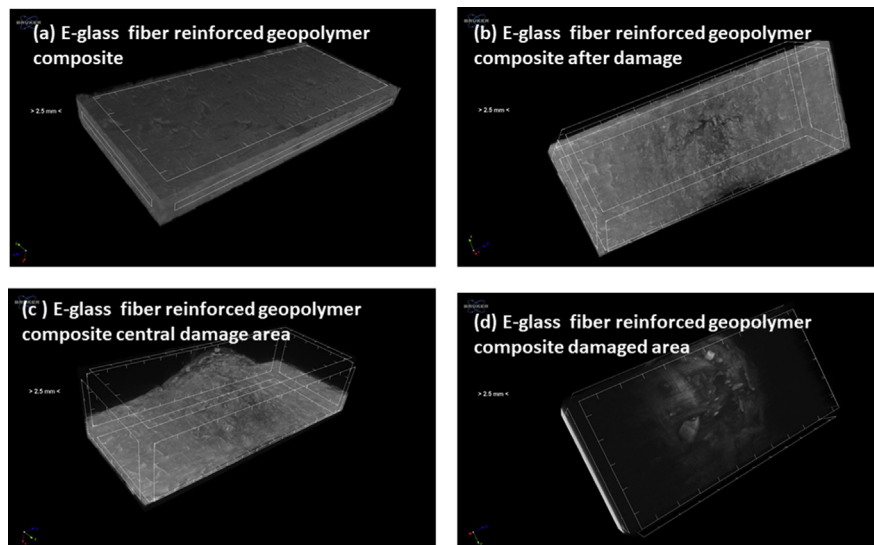

Fig. 13. (a–d) 3D image of the E-glass fiber reinforced composite and damaged carbon composite at various stage.

microscopy (SEM, ZEISS) with a voltage of 50 V. The optical microscope image of the samples was carried out by OM (NIKON EPIPHOT 200) to observe the warp and weft direction of the arrangement of fibers. Finally, 3D view of fiber without any temperature effect was carried out to investigate the fiber orientation, delamination, quality of the composite (Micro CT, Bruker, Belgium). Effect of temperature on the expansion of the composite and mass retention in geopolymer composite for various fibers is determined [20, 21].

3. Results

3.1. Physical properties of the matrix, fiber and fiber reinforced geopolymer composite at room temperature

The behavior of the matrix as the function of temperature is investigated by differential scanning calorimetry. The DSC curve of the geopolymer composite matrix at room temperature exhibits two exothermic peaks as the function of temperature at 101 and 248 °C. The first peak at 101 °C contributes to evaporation of water vapor, dehydration, and gases from the geopolymer matrix. The second peak contributes to 248 °C to mass loss of the geopolymer matrix [22].

3.2. Sustainability of fiber reinforced geopolymer composite after exposure to various temperature

The composite with fabrics such as carbon, E-glass, and basalt was exposed at various temperatures such as RT, 200, 400, 600, 800 and 1000 °C within a definite period of time inside the oven. The evolution of microstructure at each individual temperature was examined and the observation of fiber sustainability within the composite was observed. The bonding between fiber and matrix was developed as the function of temperature. The volume fraction of fiber and matrix as the function of temperature was evaluated by the simple rule of mixture. The survival strategy of fiber with respect to temperature as well as matrix behavior determines the overall strategies of the composite at higher temperature [23, 24]. Also, the developing of cracks, voids, damage, breakage of the fiber during exposure to high temperature contributes towards sustainability of composite at a respective temperature [25, 26].

Fig. 1 shows the geopolymer matrix and its respective fiber reinforced geopolymer composite at room temperature. At 200 °C, the fibers oriented as the ratio of packing density factor of the matrix in the composite. Fewer pores and voids are developed may be due to dehydration of water and evaporation of gases from the composite (Fig. 2). The necking and
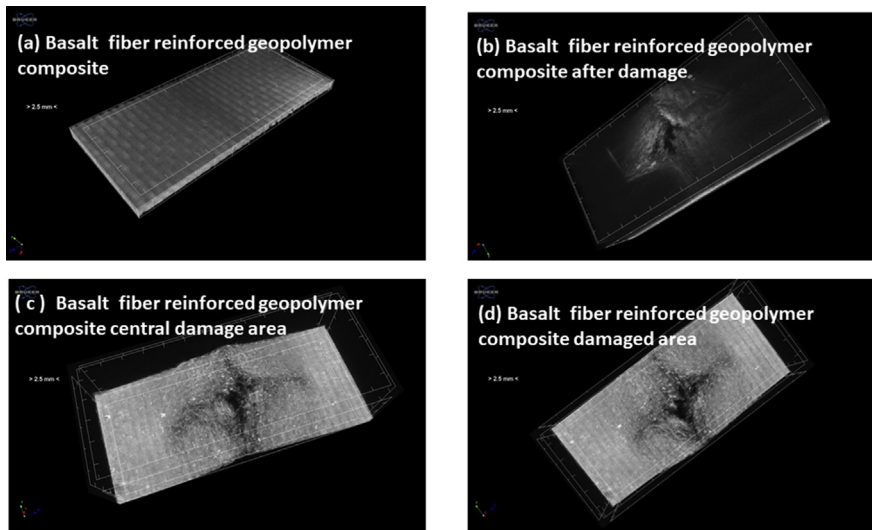
Fig. 14. (a–d) 3D image of the basalt fiber reinforced composite and damaged carbon composite at various stage.
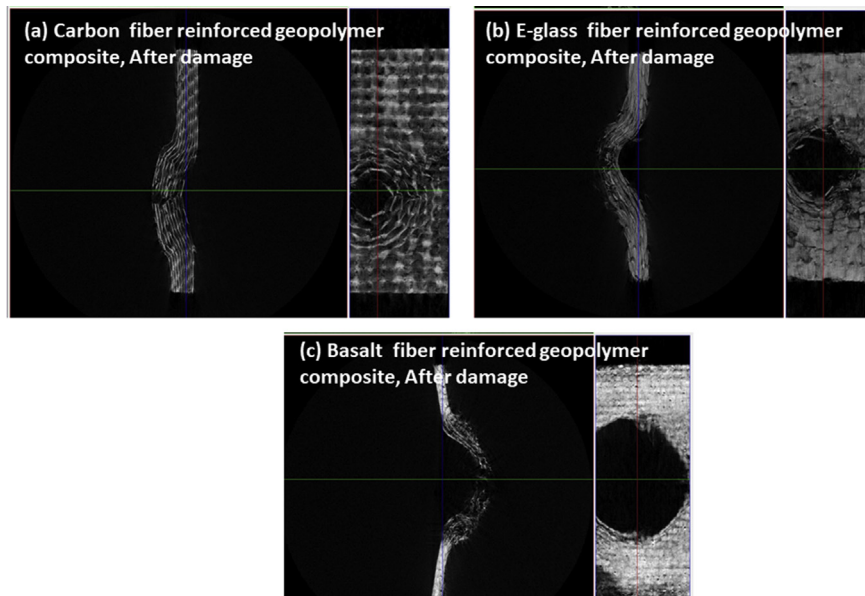

Fig. 15. Fiber breakage examination at damage area in carbon, E-glass and basalt fiber reinforced composite.

formation of bonding between fiber and matrix develop in this range of temperature, as a result, a compact form of the composite formed (Fig. 3). Carbon fiber shows a maximum strength compared to E-glass and basalt fiber (Tables 2a and 2b) [27, 28, 29]. Similarly, carbon geo-composite shows maximum flexural strength until the strain of 2 % [30, 31]. However, the slipping mechanism is observed in E-glass geo-composite until the strain of 3 %. Carbon and basalt geo-composite shows sharp failure point after the flexural strength [32, 33].

The evolution of ceramic like structure develops in basalt reinforced geopolymer composite (Fig. 4). Some breakage of carbon fibers observed in this temperature range may be more shrinkage of the composite as the function of fiber loss is observed [34, 35, 36]. It has been observed that carbon and E-glass fiber survives until 600 °C. On increasing temperature thermal expansion of E-glass fiber arises, that contributes towards the expansion of E-glass composite at 800 °C, with cage like structure develops in overall composite [37, 38, 39]. Porosity was observed in basalt composite and carbon fiber reinforced composite shows more homogeneity of the matrix and fiber orientation (Fig. 5). The complete conversion of the ceramic structure was developed in basalt reinforced

composite, and E-glass shows expansion of fibers from the room temperature with voids leading to non-adhesion between fiber and matrix develops. However, carbon fiber reinforced composite shows well homogenized oxide layer formation in the composite (Fig. 6).

3.3. Evolution of adhesion bonding between fiber-matrix in geopolymer at a higher temperature

Fig. 7 show the various fiber and matrix evolution with temperature. At 200 °C, carbon fiber shows partly disintegration in fiber with core highlighted. However, E-glass and basalt show intact in position and better adhesion within the matrix. Geopolymer matrix shows a good surface with less porosity (Fig. 7 d). At 400 °C, basalt, carbon and E-glass fiber shows adherence of fiber in a matrix of the composite. The matrix of geopolymer shows condensation towards agglomeration of a particle in the matrix (Fig. 8). On increasing temperature towards 600 °C, the fiber behaves in thickness expansion (E-glass fiber) and cracking within the fiber is observed (basalt fiber). However, carbon fiber shows shrinkage or reduced in diameter of the fiber with minor destruction in the periphery
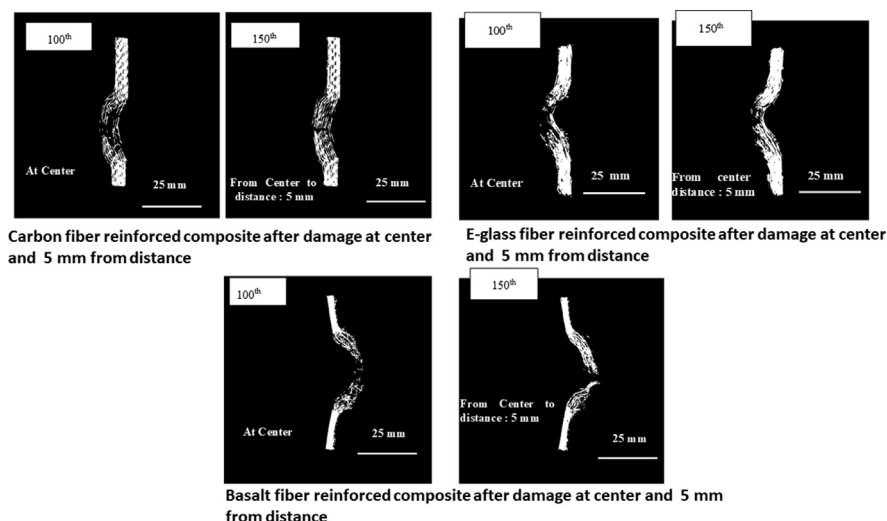
Fig. 16. Fiber breakage at center and at inner point at 5 mm distance shows the fiber breakage in carbon, E-glass and basalt fiber reinforced composite. Carbon fiber shows less fiber breakage in compare to E-glass fiber. However, the complete fiber breakage is shown in basalt fiber.

region. The matrix shows cracks in pockets within the surface (Fig. 9). The surface divides into pockets with a line of mini cracks observed in the surface. At 800 °C, the micro and mini pores are observed within the periphery of basalt fiber. However, carbon fiber shows some fragmentation within the matrix with fiber shape remain in a position [40, 41, 42]. E-glass fiber shows large dislocation within the spacing of the fibers along the normal direction that leads towards delamination within the fiber. However, the matrix shows more stable with mini cracks in the pockets of the surface, with swelling appears (Fig. 10). The matrix shows melting behavior with a viscosity in the glassy region towards the more stabilized structure. However, the survival period of the composite with carbon fiber is for a limited time. The definite period of time contributes to the strength and life period of the composite material at high temperature [43, 44]. However, the basalt reinforced composite is more brittle in nature and ceramic like structure. E-glass reinforced composite shows wafer like structure with networking cage like structure, shows no strength in the matrix. The matrix of the geopolymer begins to melt at 1000 °C and carbon fiber reinforced geopolymer composite shows the formation of oxide layers on the surface of the composite (Fig. 11) [45].

3.4. 3D characterization of geopolymer composite and damaged geopolymer composite

Fig. 12 shows 3D characterization of carbon fiber reinforced composite and the internal structure of the geopolymer composite after damage. The internal structure was investigated by micro computed tomography method and its 3D image was reconstructed using the program Voxel software. The composite before damage and after damage with various locations of damage shows fiber breakage and matrix rupture in the central damage area. Similarly, Fig. 13 shows the E-glass fiber reinforced composite and its internal structure before and after damage. E-glass composite shows damage in central point the fiber breakage and matrix rupture, however overall the composite shows loose structure that may be due to sliding nature of E-glass fiber within the matrix of the composite. The poor adhesion between fiber and matrix is observed in the overall composite. The sliding nature of E-glass fiber within the matrix of the geopolymer composite results in less damage in the overall of the composite. However, the basalt fiber reinforced composite shows good adhesion between fiber and matrix of the composite (Fig. 14 a). The severe damage was observed in the central area, resulting in voids in the composite (Fig. 14 b–d). The drop in weight with an indent for damage shows a wide gap in the central region. On comparison with various fiber reinforced composites, the composites were analyzed on the fiber

breakage at central damage area of the three composites (Fig. 15). This shows carbon fiber stands well, only inducing a notch in damage area, E-glass fiber also survives well with an upper surface notch. However, basalt fiber shows sever breakage and complete destruction in the central area. There is a wide gap, a complete void/gap at the center is visible. Fig. 16 shows the fiber damage at the center and from the 5 mm to the center for carbon, E-glass and basalt fiber reinforced composite. The remains of carbon and E-glass fiber exist in geopolymer composite, however, basalt fiber shows complete breakage at the center and inner part of the composite [46].

4. Discussion

Geopolymer minerals show the evolution of minerals from the precursors such as metakaloin binder and Na or K hydroxide on exposure to thermal treatment. As a result, the ration of Si/Al content has a strong influence on the thermal behaviour such as shrinkage or cracking in the geopolymer matrix. This was attributed towards denification of the matrix with less porosity. According to previous literature geopolymers with a high Al/Si ratio shows thermal stability up to 1300–1400 °C.

The fiber reinforced geopolymer composite on exposure to high temperature shows evaporation of hydroxide and gases induce more crystalline phase. The crystallisation of dense sodium aluminosilicate phases namely nepheline was formed at temperature 800 °C in the case of metakaolin geopolymer. The decrease in the quantity of the amorphous phases from 66% to 43% results at 1000 °C. This might be due to the conversion of crystallisation into nepheline ($NaAlSiO4$) and anortoclase ($NaAlSi3O8$). Mineral phases such as quartz, hematite, and maghemite were likely reduced in intensity that signifies towards a decrease in the quantity. These phases have higher melting points than 1000 °C. However, mullite and quartz (β-cristobalite) have melting temperatures of 1830 °C and 1713 °C respectively.

5. Conclusions

Survival of fiber reinforced geopolymer composites at various temperature was described until the final failure happens. This observation provides details behavior of fiber and matrix at RT and also towards the elevated temperature of 1000 °C. The thermal and mechanical analysis shows the strength of carbon fiber reinforced composite sustain upon a definite period of time. The expansion, breakage, cracks, delamination was observed as the function of temperature. E-glass and basalt fiber reinforced composite shows failure in strength and less survival strategy

at a higher temperature. Basalt fiber reinforced composite shows ceramic structure conversion as a result sample converts to brittle in nature. However, carbon fiber reinforced composite shows the formation of a protective oxide layer on the exposure to high temperature. That helps in better survival strategy at elevated temperature with a strength of the material.

Declarations

Author contribution statement

Sneha Samal: Conceived and designed the experiments; Performed the experiments; Analyzed and interpreted the data; Contributed reagents, materials, analysis tools or data; Wrote the paper.

Funding statement

Competing interest statement

The authors declare no conflict of interest.

Additional information

No additional information is available for this paper.

References

[1] J. Davidovits, Geopolymers: inorganic polymeric new materials, J. Therm. Anal. 37 (1991) 1633–1656.

[2] P. Duxson, A. Fernández-Jiménez, J. Provis, G. Lukey, A. Palomo, J.S.J. van Deventer, Geopolymer technology: the current state of the art, J. Mater. Sci. 42 (2007) 2917–2933.

[3] R. Embong, A. Kusbiantoro, N. Shafiq, M.F. Nuruddin, Strength and microstructural properties of fly ash based geopolymer concrete containing high-calcium and water-absorptive aggregate, J. Clean. Prod. 112 (2016) 816–822.

[4] P. He, D. Jia, T. Lin, M. Wang, Y. Zhou, Effects of high-temperature heat treatment on the mechanical properties of unidirectional carbon fiber reinforced geopolymer composites, Ceram. Int. 36 (2010) 1447–1453.

[5] W.M. Kriven, Geopolymer based composites, Encycl. Compr. Compos. Mater. II 5 (2018) 269–280.

[6] G. Mucsi, Á. Szenczi, S. Nagy, Fiber reinforced geopolymer from the synergetic utilization of fly ash and waste tire, J. Clean. Prod. 178 (2018) 429–440.

[7] A. Natali, S. Manzi, M.C. Bignozzi, Novel fiber reinforced composite materials based on sustainable geopolymer matrix, Proc. Eng. 21 (2011) 1124–1131.

[8] R.M. Novais, J. Carvalheiras, M.P. Seabra, R.C. Pullar, J.A. Labrincha, Effective mechanical reinforcement of inorganic polymers using glass fiber waste, J. Clean. Prod. 166 (2017) 343–349.

[9] S. Samal, M. Kolinova, I. Blanco, The magneto-mechanical behavior of active components in iron-elastomer composite, J. Compos. Sci. 2 (3) (2018) 54.

[10] Sneha Samal, Jarmil Vlach, Marcela Kolinova, Pavel Kavan, Micro-computed tomography characterization of isotropic filler distribution in magnetorheological elastomeric composites, in: T. Ohji, M. Singh, M. Halbig, K. Moon (Eds.), Advanced Processing and Manufacturing Technologies for Nanostructured and Multifunctional Materials, 2017/1/4, pp. 57–69.

[11] I. Perná, T. Hanzlíček, The solidification of aluminum production waste in geopolymer matrix, J. Clean. Prod. 84 (2014) 657–662.

[12] S. Samal, N.P. Thanh, I. Petríková, B. Marvalová, Improved mechanical properties of various fabric reinforced geocmposite at elevated temperature, J. Metal 67 (7) (2015) 1478–1485.

[13] S. Samal, B. Marvalová, I. Petríková, K.A.M. Vallons, S.V. Lomov, H. Rahier, Impact and post impact behavior of fabric reinforced geopolymer composite, Constr. Build. Mater. 127 (2017) 111–124.

[14] S. Samal, D. Reichmann, I. Petrikova, B. Marvalova, Low velocity impact on fiber reinforced geocomposites, Appl. Mech. Mater. 827 (2016) 145–148.

[15] H. Celerier, J. Jouin, V. Mathivet, N. Tessier-Doyen, S. Rossignol, Composition and properties of phosphoric acid-based geopolymers, J. Non Crystal. Sol. 493 (1) (2018) 94–98.

[16] D. Kong, J. Sanjayan, Damage behavior of geopolymer composites exposed to elevated temperatures, Cement Concr. Compos. 30 (2008) 986–991.

[17] S. Samal, N.P. Thanh, B. Marvalova, I. Petrikova, Thermal characterization of metakaolin-based geopolymer, JOM (2017) 1–5.

[18] S. Samal, N.P. Thanh, I. Petríková, B. Marvalová, K.A.M. Vallons, S.V. Lomov, Correlation of microstructure and mechanical properties of various fabric reinforced geopolymer composites after exposure to elevated temperature, Ceram. Int. 41 (9) (2015) 12115–12129.

[19] S. Samal, M. Kolinova, H. Rahier, I. Blanco, Micro computed characterization of geo polymer composite under mechanical load, Appl. Sci. (2018).

[20] H. Xu, J.S.J. Van Deventer, The geopolymerisation of alumino-silicate minerals, Int. J. Miner. Process. 59 (2000) 247–266.

[21] F.J. Silva, C. Thaumaturgo, Fiber reinforcement and fracture response in geo polymeric matrices, Fatigue Fract. Eng. Mater. Struct. 26 (2006) 167–172.

[22] Y.J. Zhang, S. Li, Y.C. Wang, D.L. Xu, Microstructural and strength evolutions of geopolymer composite reinforced by resin exposed to elevated temperature, J Non Crystall. Sol. 358 (1) (2012) 620–624.

[23] M. Arnoult, M. Perronnet, A. Autef, S. Rossignol, How to control the geopolymer setting time with the alkaline silicate solution, J. Non Crystall. Sol. 495 (1) (2018) 59–66.

[24] Sneha Samal, Marcela Kolinova, Hubert Rahier, Giovanni Dal Poggetto, I. Blanco, Investigation of the internal structure of fiber reinforced geopolymer composite under mechanical impact: a micro computed tomography (μCT) study, Appl. Sci. 9 (3) (2019) 516, 9 (3), 516-530.

[25] R.E. Lyon, P.N. Balaguru, A. Foden, U. Sorathia, J. Davidovits, Fire-resistant aluminosilicate composites, Fire Mater. 21 (1997) 67–73.

[26] T. Bakharev, Durability of geopolymer materials in sodium and magnesium sulfate solutions, Cement Concr. Res. 35 (2005) 1233–1246.

[27] A. Buchwald, H. Hilbig, C. Kaps, Alkali-activated metakaolin-slag blends - performance and structure in dependence of their composition, J. Mater. Sci. 42 (9) (2007) 3024–3303.

[28] D.L.Y. Kong, J.G. Sanjayan, Effect of elevated temperatures on geopolymer paste, mortar, and concrete, Cement Concr. Res. 40 (2) (2010) 334–339.

[29] A. Palomo, M.W. Grutzeck, M.T. Blanco, Alkali-activated fly ashes: a cement for the future, Cement Concr. Res. 29 (8) (1999) 1323–1329.

[30] F. Lolli, H. Manzano, J.L. Provis, M.C. Bignozzi, E. Masoero, Atomistic simulations of geopolymer models: the impact of the disorder on structure and mechanics, ACS Appl. Mater. Interfaces (2018).

[31] A. Koleżyński, M. Król, M. Żychowicz, The structure of geopolymers–Theoretical studies, J. Mol. Struct. 1163 (2018) 465–471.

[32] T. Bakharev, Thermal behaviour of geopolymers prepared using class F fly ash and elevated temperature curing, Cement Concr. Res. 36 (2006) 1134–1147.

[33] V. Barbosa, K. McKenzie, Thermal behavior of inorganic polymers and composites derives from sodium polysialate, Mater. Res. Bull. 38 (2003) 319–331.

[34] T.W. Cheng, J.P. Chiu, Fire-resistant geopolymer produced by granulated blast furnace slag, Miner. Eng. 16 (2003) 205–210.

[35] J. Giancaspro, P. Balaguru, R. Lyon, Use of inorganic polymer to improve the fire response of balsa sandwich structures, J. Mater. Civ. Eng. 18 (3) (2006) 390–397.

[36] I. Giannopoulou, D. Panias, Fire resistant geopolymers synthesized from industrial wastes, World J. Eng. 5 (3) (2008) 130–131.

[37] M. Guerrieri, J. Sanjayan, Behavior of combined fly ash/slag-based geopolymers when exposed to high temperatures, J. Fire Mater. 34 (2010) 163–175.

[38] T.D. Hung, P. Louda, D. Kroisova, O. Bortnovsky, N.T. Xiem, New generation of geopolymer composite for fire-resistance, in: Dr. Pavla Tesinova (Ed.), Advances in Composite Materials – Analysis of Natural and Man-Made Materials, InTech, 2011, pp. 73–94.

[39] D. Kong, J. Sanjayan, K. Sagoe-Crentsil, Comparative performance of geopolymers made with metakaolin and fly ash after exposure to elevated temperatures, Cement Concr. Res. 37 (2007) 1583–1589.

[40] S. Samal, M. Stuchlík, I. Petrikova, Thermal behavior of flax and jute reinforced in matrix acrylic composite, J. Therm. Anal. Calorim. 131 (2) (2018) 1035–1040.

[41] D. Kong, J. Sanjayan, Effect of elevated temperatures on geopolymer paste, mortar, and concrete, Cement Concr. Res. 40 (2010) 334–339.

[42] R.E. Lyon, et al., Fire resistant aluminosilicate composites, Fire Mater. 21 (1997) 67–73.

[43] Z. Pan, J.G. Sanjayan, B. V Rangan, An investigation of the mechanisms for strength gain or loss of geopolymer mortar after exposure to elevated temperature, J. Mater. Sci. 44 (2009) 1873–1880.

[44] K. Sakkas, P. Nomikos, A. Sofianos, D. Panias, Slag Based Geopolymer for Passive Fire protection of Tunnels, World Tunnel Congress 2013, Geneva, 2013a, pp. 343–349.

[45] K. Sakkas, P. Nomikos, A. Sofianos, D. Panias, Inorganic polymeric materials for passive fire protection of underground constructions, Fire Mater. 37 (2013b) 140–150.

[46] R. Zhao, J.G. Sanjayan, Geopolymer and Portland cement concretes in simulated fire, Mag. Concr. Res. 63 (2011) 163–173.